

Inkjet-Printed Random Lasers

Yu-Ming Liao, Wei-Cheng Liao, Shu-Wei Chang, Cheng-Fu Hou, Chia-Tse Tai, Chen-You Su, Yun-Tzu Hsu, Min-Hsuan Wu, Rou-Jun Chou, Yao-Hsuan Lee, Shih-Yao Lin, Wei-Ju Lin, Cheng-Han Chang, Golam Haider, Monika Kataria, Pradip Kumar Roy, Krishna Prasad Bera, Christy Roshini Paullinbaraj, Han-Wen Hu, Tai-Yuan Lin, and Yang-Fang Chen*

Printing technology has led to a multitude of revolutions in design, conception, fabrication, and application of optoelectronics nowadays especially for wearables and one-off devices. Recent advances range from solar cells, batteries, sensors, LEDs, displays, biomedical widgets to smart tags. Inkjet-printed random lasers (IPRLs), demonstrated here, fill in the crucial but missing piece of the puzzle in printed optoelectronics as well as progress in laser research. A broad emission spectrum of IPRL inks covering more than 75% gamut of CIE color space is successfully exploited and well adopted by commercial desktop inkjet printers. Furthermore, based on the digital, ink-efficient, mask-free patterning, and drop-on-demand printing technique, a series of long-anticipated proofs-of-concept including on-chip laser lighting modules, red-yellow-green-blue pixel-based laser displays, and ink-crypto/laser-coded security printing technique are also demonstrated.

Printing technology, nowadays, is beyond the texts, graphics, and colors. Such old embryonic invention has evolved from being just a tool for visual information needs into a generator

for functionalities.^[1,2] Traditional silicon-based devices are mainly manufactured by photolithography, vacuum deposition, and electroless plating processes. However, all these methods suffer from several drawbacks, for example, multi-staged procedures, high-cost investment, and undesirable polluting waste. As alternatives, printing techniques, including spin-coating, doctor-blading, screen printing, gravure printing, flexographic printing, roll-to-roll printing, and inkjet printing, create a lean, secure, and efficient manufacturing way to integrate solution-based inorganic/organic/biological materials with a wide range of substrates from papers, plastics to textiles or otherwise.^[3] Among these, inkjet printing, which can digitally deposit

concocted inks into prescribed arrangements with the non-impact, maskless approach, and minimal material wastage has aroused considerable attention.^[4–9] Moreover, this digital printing technique with great versatility, adaptivity, and universality promises not only high potential for industries to import inkjet printing into existing production lines but also unprecedented opportunities for broader audiences to design and customize do-it-yourself (DIY) optoelectronics just in office or household. To date, various kinds of inkjet-printed functional devices have been realized, such as LEDs,^[10,11] displays,^[12–14] transistors,^[15–17] sensors,^[18–20] solar cells,^[21,22] integrated smart systems,^[23,24] etc.^[25]


Laser, undoubtedly, is the indispensable tool in our daily life for communicating, manufacturing, entertainment, and medical treatment. Nevertheless, to integrate printing technique with conventional laser system is challenging due to the requirement of rigid resonator cavities with meticulous precision manufacturing and specific limited materials. On the other hand, the random laser system is a potential candidate. Random lasing actions occur when the photons via multiple scattering in the disordered materials let the gain surpass the loss,^[26] viz., such mirror-free laser systems can be more easily fabricated by the time-saving and cost-effective printing procedures. Besides, significant efforts have been made to realize random lasers in diversified materials from inorganic/organic to biological system,^[27–33] spanning a wide range of wavelength

Y.-M. Liao, W.-C. Liao, S.-W. Chang, C.-T. Tai, C.-Y. Su, Y.-T. Hsu, M.-H. Wu, R.-J. Chou, Y.-H. Lee, S.-Y. Lin, W.-J. Lin, C.-H. Chang, Dr. G. Haider, M. Kataria, P. K. Roy, K. P. Bera, C. R. Paullinbaraj, H.-W. Hu, Prof. Y.-F. Chen
Department of Physics
National Taiwan University
Taipei 106, Taiwan
E-mail: yfchen@phys.ntu.edu.tw

Y.-M. Liao, K. P. Bera, C. R. Paullinbaraj
Nanoscience and Technology Program
Taiwan International Graduate Program
Academia Sinica
Taipei 115, Taiwan

C.-F. Hou, Prof. T.-Y. Lin
Institute of Optoelectronic Sciences
National Taiwan Ocean University
Keelung 202, Taiwan

M. Kataria
Molecular Science and Technology Program
Taiwan International Graduate Program
Academia Sinica
Taipei 115, Taiwan

 The ORCID identification number(s) for the author(s) of this article can be found under <https://doi.org/10.1002/admt.201800214>.

DOI: 10.1002/admt.201800214

from ultraviolet to near-infrared and even to terahertz.^[34] This strong database provides numerous practical examples and universal solutions for following researchers to exploit random laser system with existing printing techniques and facilities. It is also worth mentioning that random lasers hold several amazing features, such as dexterity, transferability, tunability, flexibility, stretchability, self-healability, recyclability, and transient capability,^[30,31,35–40] which are desirable for wearables, one-off gadgets, and Internet of Things (IoTs), yet quite difficult to achieve in conventional lasers. Moreover, random laser with several exclusive superiorities, such as angle-free emissions, lying somewhere between lasers and common illuminants, shows high application values in laser illumination, speckle-free laser imaging, broad-angular laser displays, and integrated photonic lab-on-a-chip systems.^[26,34,41,42] We believe and foresee that such unconventional laser system can and will play a decisive and irreplaceable role in the follow-on laser technology advancements and printed optoelectronics industries.

Imagine that, in the near future, lasers can be easily printed on anything anywhere by anyone with only one desktop inkjet printer. Notably, the inkjet-printed random lasers (IPRLs) demonstrated in this work have successfully let this science fictional scenario come into reality (**Figure 1** and **Figure S1**, Supporting Information). One layer or several layers of spatially defined organic films that emit random lasers with selective colours can be deposited on the polyethylene terephthalate (PET) substrate in the prescribed arrangement by the common inkjet printer (more detailed information of inkjet printer setup is provided in the Experimental Section). A set of red-yellow-green-blue (RYGB) monochromatic inks covering a huge color gamut more than 75% of colors perceptible to human eyes have been successfully designed and concocted. Four organic laser dyes, namely, 4-dicyanomethylene-2-*tert*-butyl-6-*l*,1,7,7-tetramethyljulolidin-4-yl-vinyl-4H-pyra (DCJTb) (red), rhodamine 6G (yellow), rhodamine 110 (green), and stilbene 420 (blue) are selected to be the gain media of the inks of the IPRLs. Changing the color of the lasing action is as simple as using different colors of inks. Next, to ensure the stability and compatibility of ink formula with existent inkjet printers, an ink-based precursor for in situ synthesis of self-assembled metallic nanoparticles with minimal cost, chemical waste, and temperature requirements has been systematically introduced. Moreover, several advanced proofs-of-concept including on-chip printed laser illuminants, RYGB pixel-based laser displays, and ink-encrypted security printings are also demonstrated. In our previous work,^[42] we used direct dropping or spin-coating technique to fabricate monochromatic polymer film for on-chip laser illuminant modules. However, based on these methods, it is quite hard to realize scalable, ink-efficient, additive patterning, and drop-on-demand approaches (more discussions are included in Section S1, Supporting Information). Also, IPRLs are opening a host of possibilities for lasers in the next-generation wearable and soft optoelectronics. It is highly anticipated that IPRLs can be further applied to photonic integrated circuits for communicating and computing,^[43] opto-microfluidics for biondiagnostics and biostatistics,^[29,44,45] or smart prints for identification and authentication.^[28,46]

The motivation to introduce organic technology into IPRLs is because of several irreplaceable features including

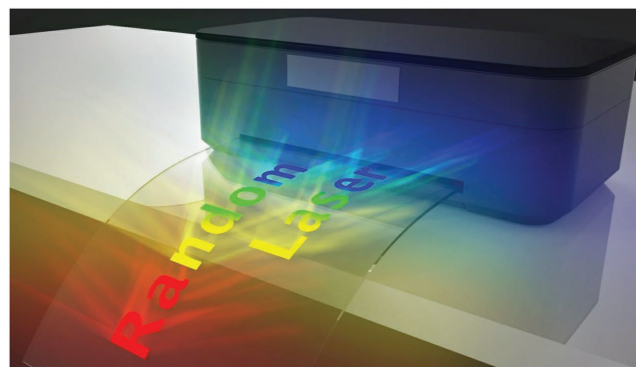


Figure 1. Schematic of the inkjet-printed random lasers (IPRLs).

low-temperature requirement, cost-competitive material, all-solution process, thin-film coating, etc.^[47,48] However, traditional methods using dielectric scatterers (photonic particles) and organic dye solutions suffer from severe competition between gain volume and high scattering efficiency.^[26,34] This problem is important because the ink output of inkjet printer is limited. In addition, dye solutions have low resistance to alterations. For example, when the inks are transferred to different mediums such as papers or plastics, the interactions between inks and substrates may lead to performance-lowering defects or uneven distribution of dyes and scatterers. Therefore, synthesis of flexible yet scalable inks with resistance to alterations are the key enablers for the realization of IPRLs.

To resolve above-mentioned problems, we develop an ameliorated in situ method as shown in **Figure 2a**. Poly(vinyl alcohol) (PVA) is added as resistance-increasing host materials and reducing agents for the synthesis of the inks incorporating self-assembled silver nanoparticles. Namely, the mixed aqueous solutions of silver nitrate (AgNO_3) and PVA are preprocessed by heating on a hot plate. During this process, PVA plays the role of reducing agents as well as solution stabilizers. As a result, the mixed solutions turn into a light-yellow precursor. We investigate the fundamental properties of the synthesized silver nanoparticles by taking transmission electron microscopy (TEM) images and measuring the absorption spectrum of the precursor. Coating pure precursor on copper mesh, the TEM images (**Figure 2b** and **Figure S2**, Supporting Information) show that silver nanoparticles are distributed evenly and randomly within the host materials. The mean diameter of silver nanoparticles is around 10 nm, which is estimated and averaged by these TEM images. The absorption spectrum of the precursor (blue curve) is shown in **Figure 2c**. A broad absorption band with a peak centered at around 410 nm is observed in the precursor. The position of the peak agrees well with the simulated localized surface plasmon spectrum (**Figure 2d**), in which we set the simulated size of silver nanoparticles in 10 nm. The relatively broad absorption band suggests that the synthesized silver nanoparticles are capable of engendering strong scattering and electromagnetic field enhancement within a wide span of wavelength.

On the other hand, DCJTb, rhodamine 6G, rhodamine 110, and stilbene 420, as active materials for RYGB lasing, are separately dissolved in deliberately selected solvents that are mutually soluble with the precursor solution. The optical

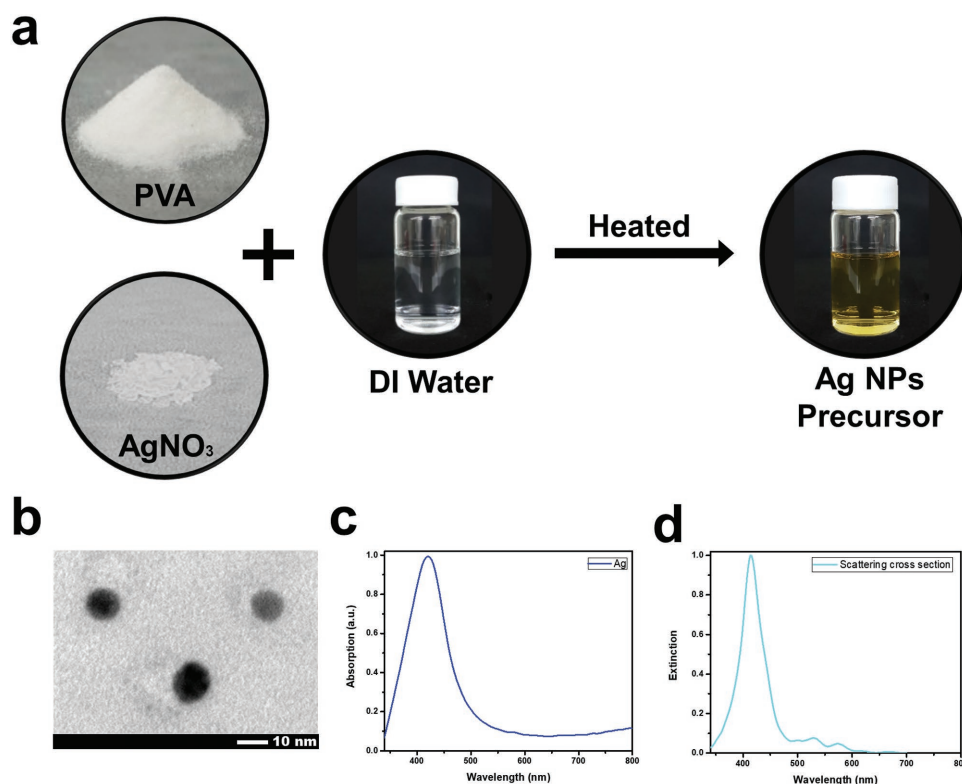


Figure 2. Solution-based silver nanoparticles precursor. a) Synthesis process, b) TEM image, c) absorption spectrum, and d) simulation of scattering cross section of silver nanoparticles precursor.

properties of these dye solutions, including photoluminescence (the solid line) and absorption spectra (the dashed line), are measured and provided in **Figure 3a–d**. The broadband photoluminescence emission spectra of RYGB inks with the full width at the half maximum (FWHM) of tens nanometers are centered at 450, 550, 585, and 660 nm, respectively. Moreover, the full range UV–vis absorption spectra of the four different laser dyes are provided next to the photoluminescence spectra. We observe that there are overlaps between the photoluminescence and absorption of dyes (**Figure 3**) and the localized surface plasmon spectra of the synthesized silver nanoparticles (**Figure 2c**). These results reveal that silver nanoparticles can serve as efficient plasmonic scattering centers in these dyes for plasmonically enhanced random lasing.^[34] In detail, three plasmonic effects should be considered. First, the scattering effect can be greatly enhanced to generate random lasing by plasmonic nanoparticles. Second, the enhancement of local electric field can lead to stronger absorption of each gain media. Third, the excitation of surface plasmons and their transformation into propagating photons can enhance the photoluminescence of laser dyes. Briefly summarizing, these effects are indeed observed in our system, yet the influence of these three effects accounts for different proportions in different laser dyes (**Figure S3** and **Section S2**, Supporting Information). Subsequently, RYGB random laser inks are prepared as the mixture of individual dye solutions and the precursor with carefully adjusted mixing ratio. These concocted inks are imported into the cartridge of an inkjet printer and deposited on PET to form multicolor IPRLs. Taking advantages of this method, active

mediums with RYGB emissive colors are included to engender lasing with a full span of colors. Besides, the compositions of the ink are carefully adjusted to optimize its performance on PET substrate. More details about the ink formulations are provided in the Experimental Section.

Random lasers can emit broad-angular light rays using disordered gain materials. In a random laser system, the resonance occurs as a result of interference between multiple scattered light rays and provides the underlying origin for coherent light signals. A threshold above which laser starts to manifest is typical when the light rays harness adequate optical gain from stimulated emission that exceeds the lost. Provided in **Figure 4a–d** are the laser emission spectra of RYGB monochromatic IPRLs printed on PET and their input–output characteristics (more detailed information of the optical measurements are provided in the Experimental Section). In the recorded emission spectra, the evolutions from spontaneous emission to random lasing are observed. The onset of random laser emissions is illustrated by sharp lasing spikes with sub-nanometer line-widths that emerge randomly on top of the emission band. Laser actions are evident as abruptly increased emission intensities and severe plunge of FWHM above critical pump fluences, as observed in the input–output diagrams. This remarkable threshold behavior validates our approach. By using tiny silver nanoparticles that serve as plasmonic scattering centers inside the inks, we managed to bestow both high optical gain and efficacious scattering at small particle sizes. Substantially, random lasers can be realized with a wide range of active materials embedded in rather limited ink

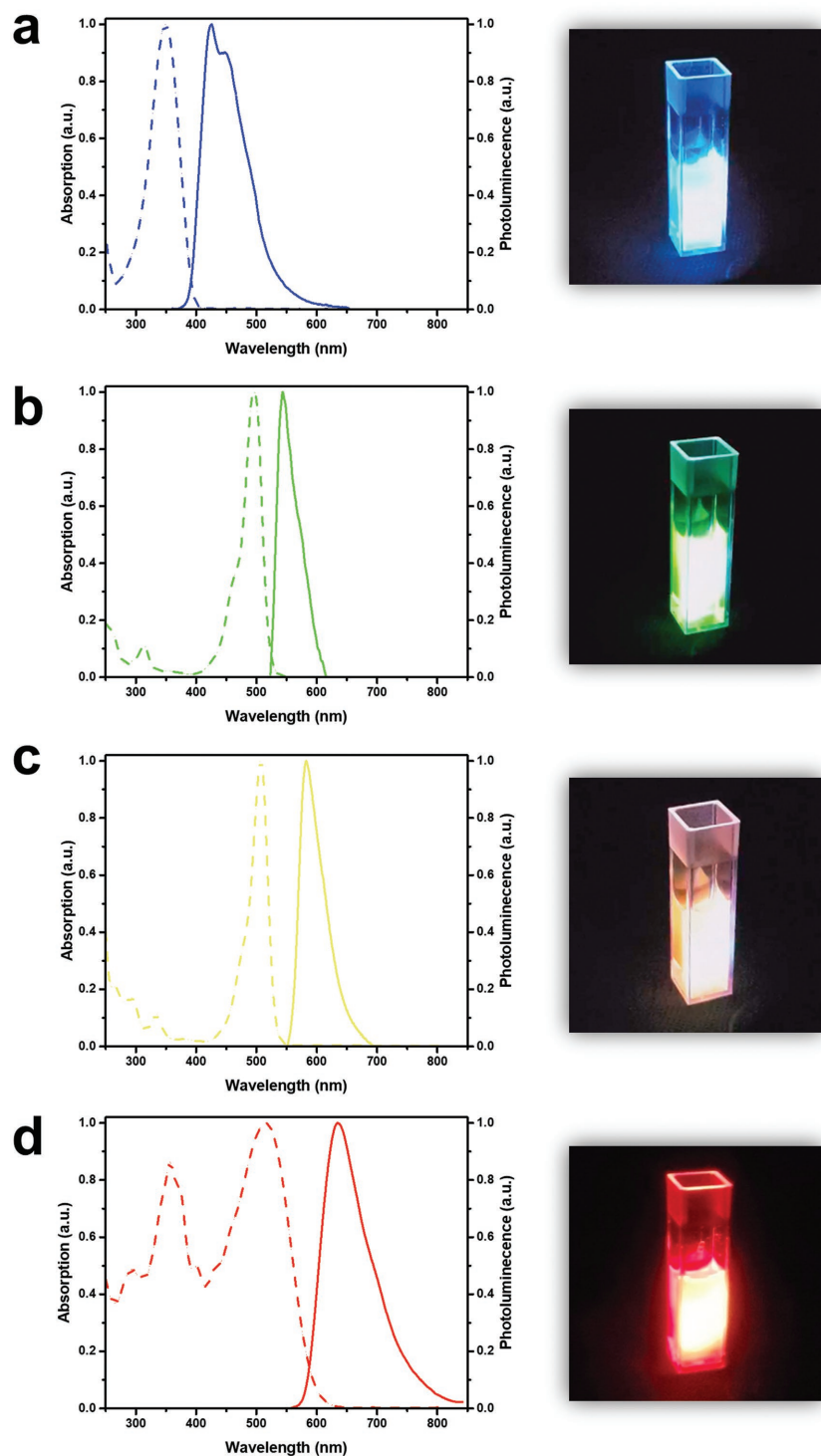


Figure 3. Characteristics of blue-green-yellow-red monochromatic laser dyes for inkjet-printed random lasers (IPRLs). a–d) The photoluminescence, absorption spectra, and corresponding images of Stilbene 420, Rhodamine 110, Rhodamine 6G, and DCJTb dye solutions, respectively.

output using this method. Based on similar disordered structures, the thresholds of RYGB IPRLs are pretty close to each other, ranging between 17 and 20 mJ cm⁻². The homogeneity guarantees a balance between different colors, which is important for pragmatic applications.

With a matrix of inkjet-printed RYGB pixels, random lasers that enable a wide span of colors can be realized, including white light. The chromaticities of RYGB IPRLs and the mixed white emission are carefully studied using luminescence spectroscopy and CIE 1931 diagram, and the corresponding photos are displayed in Figure 5a,b. In the CIE chromaticity diagram, the color space indicates the whole gamut perceptible to human eyes, and the border corresponds to the spectral colors of monochromatic light. The emissive colors of four RYGB monochromatic IPRLs are quantitatively depicted by the vertices of the quadrilateral. As shown in the diagram, the vertices locate very closely to the edge of the color space, which suggests that monochromatic IPRLs have remarkably high spectral purity. It is because of the narrow line-width of stimulated emission. As a result, the quadrilateral of RYGB IPRLs span a color gamut that covers up to 75% area of the whole perceptible color space in the CIE diagram, which is quite large in contrast to industry standard of illumination (see Figure S4, Supporting Information). Meanwhile, the chromaticity of carefully mixed white emission based on IPRLs and a D65 standard white point is displayed and compared in the diagram. By carefully adjusting the excitation power and pixel area of individual films, RYGB IPRLs could be mixed up to generate white emission that is very close to standard white light (Figure 5b).

Previous reports suggest that lasers have a great ascendancy over LEDs or traditional thermal light bulbs in display and lighting, owing to the numerous advantages, such as higher spectral purity, larger color gamut, better contrast ratio, and color saturations.^[49,50] However, such promising application is somewhat limited by the inherent directional output of laser light. As a new prototype of laser source, random lasers are different from conventional lasers since random lasers exploiting disordered structures emit stimulated output in many directions. This unique feature could allow random lasers to serve as an efficient alternative for broad-angular laser display.^[26,34,36] In Figure 5c, the pedestrian countdown display, a common traffic instruction, is demonstrated on PET substrate by the IPRLs. Displayed in Video S1 (Supporting Information), under excitation, the little green man comes alive and crosses the street within the allocated time. When the time is up, the instruction turns to a stood red man. In this IPRL-based display prototype, the light is bright and clear in different directions, and the color is vivid.

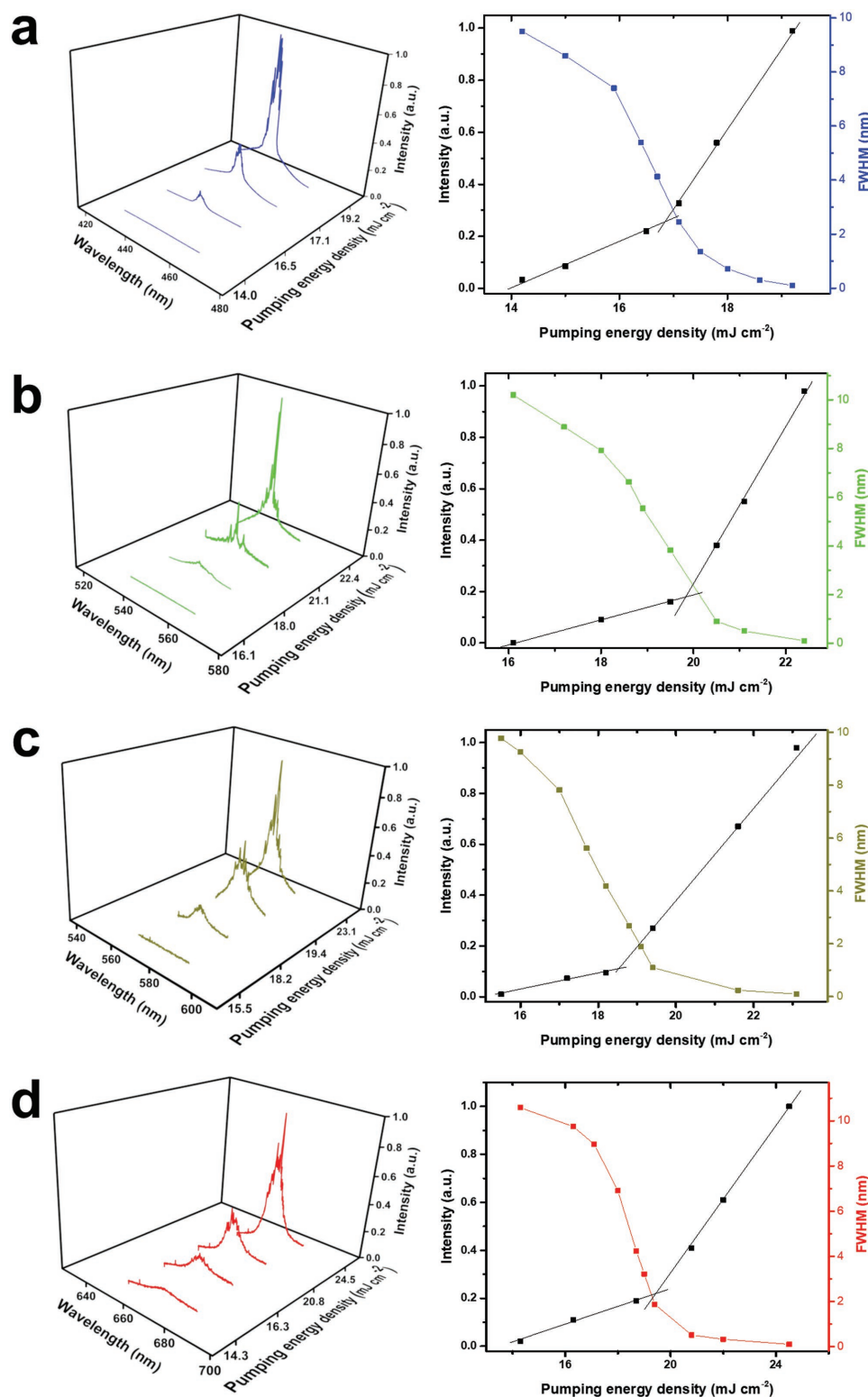


Figure 4. Performance of inkjet-printed random lasers (IPRLs). a–d) The lasing spectra, light-in-light-out curve, and full width at half maximum (FWHM) versus pumping energy density of blue, green, yellow, and red IPRLs, respectively.

This first demonstration shows that IPRLs could serve as a facile approach to not only full-color but also broad-angular laser display.

Exhilaratingly, via the individual stimulated emission spectra of the random laser, we further attempt to exploit IPRLs in security printing engineering.^[51,52] As shown in **Figure 6**, IPRLs

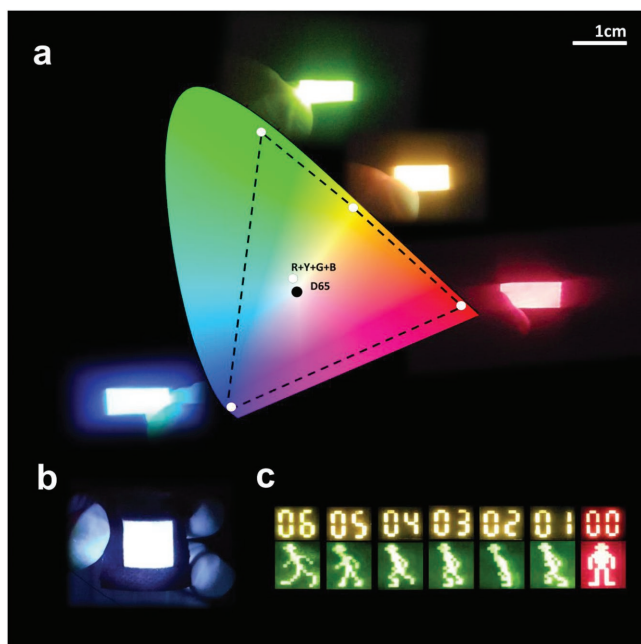


Figure 5. Proof-of-concept of inkjet-printed random lasers (IPRLs) for laser illumination and laser display. a) A CIE 1931 diagram showing the chromaticity of red, yellow, green, and blue IPRLs and their corresponding images. The mixed white emission and a standard white emission (D65) are also given. b) Photograph of white emission based on inkjet-printed red-yellow-green-blue laser pixels. c) Photographs of the inkjet-printed laser pedestrian countdown display. The corresponding video can be seen in Video S1 (Supporting Information).

can generate ink-encrypted prints and photonic barcodes/quick response (QR) codes, which can not only assist in the short-range authorization/encoding/anti-counterfeiting of signatures, documents, certificates, credit cards, and product labels but also in the long-range applications for friend-or-foe identifications, mission-to-mission interchangeable tactic-markers, and search-and-rescue communication.^[26,28,34,46,53,54] Remarkably, IPRLs could provide double-shield security protection techniques. First, these colorful prints/codes recorded by IPRLs are merely invisible at normal condition, which can only be read under laser excitation. Second,

the inks of IPRL can be concocted to perform the specific color rendering and laser characteristics only under prescribed excitation laser source and energy densities, such that predetermined read conditions become the incontrovertible laser-coded information protection. Moreover, the transient capability of IPRLs is another highlight. As soon as the mission completes, we can completely dissolve or selectively disintegrate the strictly confidential information/data under triggerable manners with controlled rates at prescribed times without no one the wiser, preventing any possibility for adversaries to collect, study, and copy. More experimental results and process of dissolvability and recyclability of IPRL inks are concluded in the Supporting Information and Experimental Section. For each color, we conduct the similar dissolving and recycling process for at least five cycles. Surprisingly, the lasing threshold, intensity, and spectra of each ink shown in Figure S5 (Supporting Information) perform a high consistency between every trial, truly achieving the possibility of dissolving and recycling IPRLs. Besides, the deformability of IPRLs is also demonstrated in Figure S6 (Supporting Information).

IPRLs with great versatility, compatibility, and universality have been systematically introduced in this work. A sequence of RYGB random laser inks covering more than 75% color gamut of the visible spectrum are exploited and well adopted by most mainstream commercial desktop printers. Furthermore, we successfully apply IPRLs for several exciting yet challenging prototype applications including on-chip laser lighting modules, RYGB pixel-based laser display, and ink-crypto anti-counterfeit prints, which are the long-awaited dreams for laser research communities over the past decades. It is believed that IPRLs proved here can significantly remedy the inherent shortcomings of laser technology nowadays and open new vistas for printed optoelectronics that people previously may not have thought possible (Section S3, Supporting Information).

Experimental Section

Solution-Based Silver Nanoparticles Synthesis: 0.5 mg silver nitrate (AgNO_3) and 1.5 g poly(vinyl alcohol) (PVA) were evenly dissolved in 100 mL deionized (DI) water. Next, the mixture was heated at 120 °C for 120 min. Finally, with this in situ reduction process, silver nanoparticles are naturally formed in this precursor solution.

Red-Ink: DCJTb was dissolved in anisole and ethanol with the ratio 4 mg:1 g:1 g. Next, the dye solution and precursor solution were mixed with the same ratio by weight.

Yellow-Ink: Rhodamine 6G was dissolved in precursor solution with the ratio 0.2 mg:1 g.

Green-Ink: Rhodamine 110 was dissolved in methanol with the ratio 1 mg:1 g by weight. Next, the dye solution and precursor solution were mixed with the ratio 1:5 by weight.

Blue-Ink: Stilbene 420 was dissolved in ethanol with the ratio 25 mg:1 g. Next, the dye solution and precursor solution were mixed with the same ratio by weight.

Inkjet Printer Setup: The inkjet printer used in this work is a Canon PIXMA G1000 Refillable Ink Tank Printer. The print resolution (dpi) is 4800 (horizontal) \times 1200 (vertical). The ISO Standard print speed (color) is 5.0 ipm. The minimum ink droplet is 2 pL, which can be found in the official

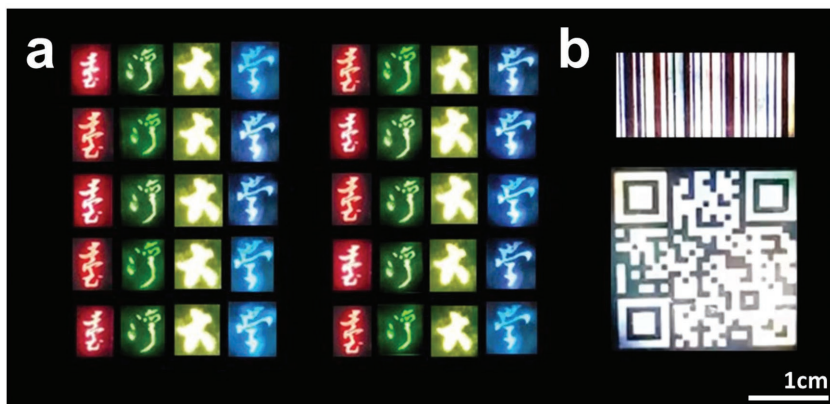


Figure 6. Inkjet-printed random lasers (IPRLs) for security printing engineering. a) Photographs of the traditional Chinese letter of National Taiwan University printed by IPRLs. b) Photographs of the ink-encrypted photonic barcodes and QR codes printed by IPRLs.

specifications manual. There are four ink cartridges enabling the printer to print four different colors simultaneously. The only modification to the inkjet printer for IPRLs was to replace the inks from Canon original equipment manufacturer with the IPRL inks concocted by the authors of this paper. Moreover, the printer heads can be ultrasonically cleaned for 10 min in selected solvents and DI water to remove the residual inks, which is a simple and straightforward maintenance methodology for the IPRL system. 3M Transparency Film PP2900 was selected as the substrates of IPRLs, which were ultrasonically cleaned for 10 min subsequently in DI water, acetone, and isopropyl alcohol (IPA) in sequence to remove any adsorbed contaminant. To prevent any unavoidable reflective radiation from the substrate and in turn to retain the real color from the IPRLs, HP Laser Jet P2015d was utilized to print a thin-layer toner on PET. The printing process was performed at room temperature. The minimum line width obtained is $\approx 3\ \mu\text{m}$ and the thickness of the pattern is $\approx 2\ \mu\text{m}$. The liquid properties of each RYGB ink, such as viscosity, surface tension, and boiling point are provided in Table S1 (Supporting Information).

Recycle Experiment of the IPRL: To test the recycling capability, the dried RYGB inks of IPRLs were immersed ultrasonically in 1 mL of DI water until the inks were totally dissolved. Next, all the solutions were dropped on the original substrates and dried at 50 °C to remove the residual water. After the emission property was recorded, they were dissolved again and the steps as described above were repeated.

Material Characterization: The silver nanoparticles were characterized by TEM (Hitachi H-7100). The absorption spectra were measured by UV-vis-NIR spectrophotometer (Perkin Elmer LAMBDA 750).

Optical Measurements: To record the random lasing emission spectra, the samples were optically excited by frequency-quadrupled 266 nm pulsed Nd:YAG laser (NewWave, Tempest 300) with 4 ns pulse width and 10 Hz repetition. The energy of single pulse shot is up to 200 mJ. The pumping beam was focused by a cylindrical lens ($f = 100\ \text{mm}$). A bandpass filter of a 20 nm width was used to block the pump laser illumination. The emission properties were spectrally analyzed using a high-resolution spectrometer Jobin Yvon iHR550 with gratings of 300 (spectral resolution 0.1 nm) and 1200 grooves mm^{-1} (spectral resolution 0.025 nm). A synapse thermoelectric cooled charge-coupled device (CCD) guaranteed to $-75\ ^\circ\text{C}$ was connected to the spectroscopy software SynerJY. Schematic view of the spectroscopic random laser setup is shown in Figure S7 (Supporting Information). All the measurements were performed at room temperature.

Numerical Simulation: The simulation result is performed using the commercial electromagnetic software (Lumerical). The refractive index of Ag is from the experimental data of Johnson and Christy,^[55] and PVA is set as 1.5.

Supporting Information

Supporting Information is available from the Wiley Online Library or from the author.

Acknowledgements

Y.-M.L., W.-C.L., and S.-W.C. contributed equally to this work. Y.-M.L., W.-C.L., S.-W.C., and C.-F.H. designed the IPRLs and developed the fabrication methods, analyzed the data, and wrote the manuscript. Y.-F.C. supervised the project and conceived the study. All authors accepted the final version of the manuscript. The authors thank Janis Liu for the visual design of IPRLs. This work was financially supported by the Advanced Research Center for Green Materials Science and Technology from The Featured Area Research Center Program within the framework of the Higher Education Sprout Project by the Ministry of Education (107L9006) and the Ministry of Science and Technology in Taiwan (MOST 107-3017-F-002-001).

Conflict of Interest

The authors declare no conflict of interest.

Keywords

inkjet-printed optoelectronics, laser display, laser illumination, random lasers, security printing

Received: June 21, 2018

Revised: August 15, 2018

Published online: September 12, 2018

- [1] M. A. Leenen, V. Arning, H. Thiem, J. Steiger, R. Anselmann, *Phys. Status Solidi A* **2009**, 206, 588.
- [2] E. MacDonald, R. Wicker, *Science* **2016**, 353, aaf2093.
- [3] S. Khan, L. Lorenzelli, R. S. Dahiya, *IEEE Sens. J.* **2015**, 15, 3164.
- [4] Z. Zhan, J. An, Y. Wei, H. Du, *Nanoscale* **2017**, 9, 965.
- [5] M. Gao, L. Li, Y. Song, *J. Mater. Chem. C* **2017**, 5, 2971.
- [6] B. J. de Gans, P. C. Duineveld, U. S. Schubert, *Adv. Mater.* **2004**, 16, 203.
- [7] M. Singh, H. M. Haverinen, P. Dhagat, G. E. Jabbour, *Adv. Mater.* **2010**, 22, 673.
- [8] F. Torrisi, T. Hasan, W. Wu, Z. Sun, A. Lombardo, T. S. Kulmala, G.-W. Hsieh, S. Jung, F. Bonaccorso, P. J. Paul, *ACS Nano* **2012**, 6, 2992.
- [9] P. Calvert, *Chem. Mater.* **2001**, 13, 3299.
- [10] S. C. Chang, J. Liu, J. Bharathan, Y. Yang, J. Onohara, J. Kido, *Adv. Mater.* **1999**, 11, 734.
- [11] T. Hebner, C. Wu, D. Marcy, M. Lu, J. Sturm, *Appl. Phys. Lett.* **1998**, 72, 519.
- [12] J. Bharathan, Y. Yang, *Appl. Phys. Lett.* **1998**, 72, 2660.
- [13] V. Wood, M. J. Panzer, J. Chen, M. S. Bradley, J. E. Halpert, M. G. Bawendi, V. Bulović, *Adv. Mater.* **2009**, 21, 2151.
- [14] E. M. Lindh, A. Sandström, L. Edman, *Small* **2014**, 10, 4148.
- [15] H. Sirringhaus, T. Kawase, R. Friend, T. Shimoda, M. Inbasekaran, W. Wu, E. Woo, *Science* **2000**, 290, 2123.
- [16] T. Kawase, H. Sirringhaus, R. H. Friend, T. Shimoda, *Adv. Mater.* **2001**, 13, 1601.
- [17] D.-H. Lee, S.-Y. Han, G. S. Herman, C.-H. Chang, *J. Mater. Chem.* **2009**, 19, 3135.
- [18] V. Dua, S. P. Surwade, S. Ammu, S. R. Agnihotra, S. Jain, K. E. Roberts, S. Park, R. S. Ruoff, S. K. Manohar, *Angew. Chem., Int. Ed.* **2010**, 49, 2154.
- [19] J. Jang, J. Ha, J. Cho, *Adv. Mater.* **2007**, 19, 1772.
- [20] B. Yoon, D. Y. Ham, O. Yarimaga, H. An, C. W. Lee, J. M. Kim, *Adv. Mater.* **2011**, 23, 5492.
- [21] C. N. Hoth, S. A. Choulis, P. Schilinsky, C. J. Brabec, *Adv. Mater.* **2007**, 19, 3973.
- [22] C. N. Hoth, P. Schilinsky, S. A. Choulis, C. J. Brabec, *Nano Lett.* **2008**, 8, 2806.
- [23] B. J. Kang, C. K. Lee, J. H. Oh, *Microelectron. Eng.* **2012**, 97, 251.
- [24] H.-Y. Tseng, V. Subramanian, *Org. Electron.* **2011**, 12, 249.
- [25] M. Edinger, D. Bar-Shalom, N. Sandler, J. Rantanen, N. Genina, *Int. J. Pharm.* **2018**, 536, 138.
- [26] D. S. Wiersma, *Nat. Phys.* **2008**, 4, 359.
- [27] H. Cao, Y. Zhao, S. Ho, E. Seelig, Q. Wang, R. Chang, *Phys. Rev. Lett.* **1999**, 82, 2278.
- [28] N. M. Lawandy, R. Balachandran, A. Gomes, E. Sauvain, *Nature* **1994**, 368, 436.
- [29] R. C. Polson, Z. V. Vardeny, *Appl. Phys. Lett.* **2004**, 85, 1289.

- [30] W.-C. Liao, Y.-M. Liao, C.-T. Su, P. Perumal, S.-Y. Lin, W.-J. Lin, C.-H. Chang, H.-I. Lin, G. Haider, C.-Y. Chang, S.-W. Chang, C.-Y. Tsai, T.-C. Lu, T.-Y. Lin, Y.-F. Chen, *ACS Appl. Nano Mater.* **2018**, *1*, 152.
- [31] H. W. Hu, G. Haider, Y. M. Liao, P. K. Roy, R. Ravindranath, H. T. Chang, C. H. Lu, C. Y. Tseng, T. Y. Lin, W. H. Shih, Y. F. Chen, *Adv. Mater.* **2017**, *29*, 1703549.
- [32] C. M. Raghavan, T.-P. Chen, S.-S. Li, W.-L. Chen, C.-Y. Lo, Y.-M. Liao, G. Haider, C.-C. Lin, C.-C. Chen, R. Sankar, *Nano Lett.* **2018**, *18*, 3221.
- [33] P. K. Roy, G. Haider, H. I. Lin, Y. M. Liao, C. H. Lu, K. H. Chen, L. C. Chen, W. H. Shih, C. T. Liang, Y. F. Chen, *Adv. Opt. Mater.* **2018**, *18*, 1800382.
- [34] F. Luan, B. Gu, A. S. Gomes, K.-T. Yong, S. Wen, P. N. Prasad, *Nano Today* **2015**, *10*, 168.
- [35] D. Wiersma, *Nature* **2000**, *406*, 132.
- [36] D. S. Wiersma, S. Cavaliere, *Nature* **2001**, *414*, 708.
- [37] B. R. Anderson, R. Gunawidjaja, H. Eilers, *Opt. Lett.* **2015**, *40*, 577.
- [38] Y. M. Liao, Y. C. Lai, P. Perumal, W. C. Liao, C. Y. Chang, C. S. Liao, S. Y. Lin, Y. F. Chen, *Adv. Mater. Technol.* **2016**, *1*, 1600068.
- [39] H. W. Hu, G. Haider, Y. M. Liao, P. K. Roy, R. Ravindranath, H. T. Chang, C. H. Lu, C. Y. Tseng, T. Y. Lin, W. H. Shih, Y. F. Chen, *ACS Nano* **2017**, *11*, 7600.
- [40] C. Y. Tsai, Y. M. Liao, W. C. Liao, W. J. Lin, P. Perumal, H. H. Hu, S. Y. Lin, C. H. Chang, S. Y. Cai, T. M. Sun, H. I. Lin, G. Haider, Y. F. Chen, *Adv. Mater. Technol.* **2017**, *2*, 1700170.
- [41] B. Redding, M. A. Choma, H. Cao, *Nat. Photonics* **2012**, *6*, 355.
- [42] S. W. Chang, W. C. Liao, Y. M. Liao, H. I. Lin, H. Y. Lin, W. J. Lin, S. Y. Lin, P. Perumal, G. Haider, C. T. Tai, K. C. Shen, C. H. Chang, Y. F. Huang, T. Y. Lin, Y. F. Chen, *Sci. Rep.* **2018**, *8*, 2720.
- [43] C. Zhang, C.-L. Zou, Y. Zhao, C.-H. Dong, C. Wei, H. Wang, Y. Liu, G.-C. Guo, J. Yao, Y. S. Zhao, *Sci. Adv.* **2015**, *1*, e1500257.
- [44] A. Smuk, E. Lazaro, L. P. Olson, N. Lawandy, *Opt. Commun.* **2011**, *284*, 1257.
- [45] K. Abe, K. Suzuki, D. Citterio, *Anal. Chem.* **2008**, *80*, 6928.
- [46] R. Balachandran, D. Pacheco, N. Lawandy, *Appl. Opt.* **1996**, *35*, 640.
- [47] M. Berggren, D. Nilsson, N. D. Robinson, *Nat. Mater.* **2007**, *6*, 3.
- [48] S. R. Forrest, M. E. Thompson, *Chem. Rev.* **2007**, *107*, 923.
- [49] A. Neumann, J. Wierer, W. Davis, Y. Ohno, S. Brueck, J. Tsao, *Opt. Express* **2011**, *19*, A982.
- [50] F. Fan, S. Turkdogan, Z. Liu, D. Shelhammer, C. Ning, *Nat. Nanotechnol.* **2015**, *10*, 796.
- [51] J. M. Meruga, A. Baride, W. Cross, J. J. Kellar, P. S. May, *J. Mater. Chem. C* **2014**, *2*, 2221.
- [52] M. You, J. Zhong, Y. Hong, Z. Duan, M. Lin, F. Xu, *Nanoscale* **2015**, *7*, 4423.
- [53] J. Martorell, R. Balachandran, N. Lawandy, *Opt. Lett.* **1996**, *21*, 239.
- [54] S. Larochelle, P. Mathieu, V. Larochelle, J. Dubois, *presented at CLEO*, Baltimore, MD, May **1997**.
- [55] P. B. Johnson, R.-W. Christy, *Phys. Rev. B* **1972**, *6*, 4370.